Surface-Enhanced Raman Scattering of 4-Aminothiophenol Adsorbed on Silver Nanosheets Deposited onto Cubic Boron Nitride Films

Yanli Zhou,*† **Jinfang Zhi,**** **Jianwen Zhao,*** **and Maotian Xu***†

  *Department of Chemistry, Shangqiu Normal University, Shangqiu 476000, P. R. China
**Key Laboratory of Photochemical Conversion and Optoelectronic Materials, Technical Institute of
  Physics and Chemistry, Chinese Academy of Sciences, Beijing 100190, P. R. China

A simple method was found for the fabrication of silver nanosheets (AgNS) by the catalysis of gold nanoparticles (AuNP) on an amine-terminated cubic boron nitride (cBN) surface deposited on a Si(001) substrate in the presence of reductant. The morphology of the AgNS/AuNP/NH$_2$-cBN/Si(001) sample was characterized by scanning electron microscopy and X-ray diffraction. The performance of the AgNS/AuNP/NH$_2$-cBN/Si(001) sample as surface-enhanced Raman scattering (SERS) active substrate was evaluated by using 4-aminothiophenol (PATP) as the probe molecule. The SERS measurements showed that the maximum intensity was obtained on the AgNS/AuNP/NH$_2$-cBN/Si(001) sample for 5 min silver deposition. Compared with the AuNP/NH$_2$-cBN/Si(001) sample and a silver film/cBN/Si(001) prepared by the mirror reaction, the SERS signal of PATP was obviously improved on the above AgNS/AuNP/NH$_2$-cBN/Si(001) film. The sensitivity and the stability of the AgNS/AuNP/NH$_2$-cBN/Si(001) sample were also investigated.

Introduction

Surface-enhanced Raman scattering (SERS) has evolved as a powerful tool for detection and identification of a wide range of adsorbate molecules due to its richness of spectral information, its high sensitivity, and its surface selectivity.[1-3] In SERS, the Raman signal intensity of a molecule gets enhanced by many orders of magnitude when it is adsorbed to metallic nanostructures with sizes on the order of tens of nanometers. The most commonly used SERS active substrates are aggregated silver and gold colloids, because of their easy preparation and high intensity enhancement in previous reports.[4-6] However, major problems of such nanoparticles in terms of stability and reproducibility limit the applications in chemical and biological analyses. Roughened metal electrodes, as another kind of common substrates, are more stable than the colloids, but they are typically not as sensitive.[7] Recently, considerable efforts have been directed to assemble the silver or gold nanostructures on glass, silicon, carbon, and metal material surfaces by many techniques including templates, vacuum evaporation, nanolithography, and etching.[8-12] The electromagnetic "hot spots" exist in the sharp features, large curvature regions, and gap sites between two particles in proximity. The above nanostructure films show significantly better stability, sensitivity, and controllability. Unfortunately, these SERS active substrates also suffer from some disadvantages, such as weak long-term stability due to instability of the substrate or desorption of metal nanostructures from the substrate surface. Therefore, the search

for reliable methods and substrate materials that can be used to prepare an efficient and reliable SERS substrate is still interesting.

On the other hand, cubic boron nitride (cBN) thin films deposited on Si(001) substrate by chemical vapor deposition (CVD) are known for high atomic density and strong covalent bonds, which make them conspicuous materials with outstanding properties including high hardness, high oxidation stability, and good chemical inertness.[13-16] cBN/Si(001) films are potentially ideal substrate materials for various chemical or biological sensing applications, whereas the application of the cBN/Si(001) thin film is scarce, except for some applications in protective coatings and cutting tools, because of the difficulty in surface modification. Recently, we firstly reported that an cBN/Si(001) surface could be functionalized by a photochemical reaction to form an amine-terminated surface.[17] Subsequently, a gold nanoparticles (AuNP) monolayer was self-assembled on the amine-terminated surface, and a dense and well-distributed AuNP monolayer was obtained. It has been reported that the AuNP could initiate the silver deposition in a silver enhancer solution in the presence of reductant, ultimately resulting in the formation of silver nanostructures by an electroless process.[18,19] The silver nanostructures-modified cBN/Si(001) surface is expected to be a SERS active substrate with high stability and sensitivity. To our knowledge, the SERS active substrates based on the cBN/Si(001) thin film have not yet been developed.

In this study, we report a simple method for the fabrication of silver nanosheets (AgNS) on AuNP/NH$_2$-cBN/Si(001) surface, which was used as an effective SERS active substrate. The nanosheets were deposited in the catalysis of AuNP on the NH$_2$-cBN/Si(001) surface by the reduction of hydroquinone. 4-Aminothiophenol (PATP) was used as Raman probe to

---

† To whom correspondence should be addressed.
E-mail: ylzhou1981@yahoo.com.cn; xumaotian@sqnc.edu.cn
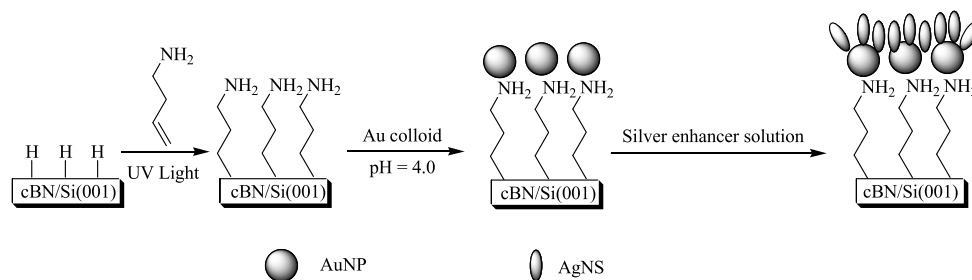
Scheme 1   Schematic illustration of the process used to fabricate the AgNS/AuNP/NH$_2$-cBN/Si(001) surface.

examine the effects of the deposition time, the sensitivity, and the stability for the prepared AgNS/AuNP/NH$_2$-cBN/Si(001) sample.

Experimental

Reagents and chemicals

Allylamine, aurichloric acid, silver acetate, and PATP were purchased from Sigma-Aldrich and were used without further purification. The other chemicals were all reagent grade. The water used throughout this work was ultrapure water (18 MΩ cm) produced by a Millipore M-Q purification system.

Apparatus

The surface morphologies of the AgNS/AuNP/NH$_2$-cBN/ Si(001) film and other prepared samples were observed by scanning electron microscopy (SEM, Philips FEG XL30). The X-ray diffraction (XRD) measurements were performed on a Philips X'Pert diffractometer using Cu K$_\alpha$ radiation. SERS spectra were measured on a Renishaw 1000 Raman spectrometer with a He–Ne laser (633 nm) as an excitation source. The acquisition time was 10 s and the resolution of the beam diameter for Raman spectroscopy was about 1 μm.

Preparation of the AgNS/AuNP/NH$_2$-cBN/Si(001) sample

cBN films were deposited on Si(001)/diamond substrates by a fluorine-assisted electron-cyclotron-resonance microwave-plasma CVD process using a gas mixture of He–Ar–N$_2$–BF$_3$–H$_2$.[15-17] The cBN/Si(001) films were modified with AgNS in three steps. Firstly, a 20-μL volume of allylamine was placed onto the cBN/Si(001) (A = 1 cm^2) surface in a N$_2$-purged Teflon reaction chamber covered with a quartz window and the material was irradiated with a UV lamp (254 nm) for 12 h. Secondly, the sample was immersed into the gold colloid solution (pH 4.0) for 24 h, rinsed with deionized water. Lastly, the above resulting surface was treated with a silver solution, which was composed of equal amounts of 0.22% silver acetate and 1% hydroquinone in 0.1 M citrate buffer (pH 4.0) under vigorous stirring.

SERS measurements of PATP on the AgNS/AuNP/NH$_2$-cBN/Si(001) film

PATP solution was diluted to different concentrations ranging from 100 to 0.1 nM with ethanol. Ten microliters of each solution were dropped onto the prepared sample, and the solvent was allowed to evaporate under ambient conditions. In this experiment, 5 SERS active substrates of each sample and 10 different points on each substrate were selected to detect the PATP probe, and the mean result was described.

Results and Discussion

Fabrication and characterization of the AgNS/AuNP/NH$_2$-cBN/ Si(001) film

The steps involved in the fabrication of the AgNS/AuNP/ NH$_2$-cBN/Si(001) films are shown in Scheme 1. Amine-terminated active cBN/Si(001) surface was obtained by the photochemical reaction between hydrogen-terminated cBN/Si(001) surface and allylamine.[17] A layer of AuNP was self-assembled on the amine-terminated cBN/Si(001) surface. A dense and well-distributed AuNP monolayer was formed. The silver deposition was further carried out by inserting the AuNP/NH$_2$-cBN/Si(001) surface into silver solution (0.1 M citrate buffer, pH 4.0). Figure 1 shows the representative SEM images of the silver deposition by the reduction of hydroquinone for different times. Owing to the promotion of AuNP, a high-density and cross-linked AgNS monolayer was observed even after a short time (10 s). The formed AgNS grew thicker with increasing exposure to the silver solution (Figs. 1a – 1d), and interestingly, the AgNS all exhibited different growth directions. Indeed, after 5 min of exposure to the silver solution, the AgNS remained unaffected in terms of size and shape, but the amount of nanosheets increased with increasing the exposure time. In addition, the AgNS could not be obtained in any other buffer solution or at any other pH (pH >5.5 or <2.5). The result demonstrated that the citrate buffer solution (2.5 < pH < 5.5) is important in the formation of AgNS.

For the sample after 5 min exposure, the high-magnification SEM image and XRD pattern are illustrated in Figs. 2a and 2b, respectively. The size of AgNS was 100 – 200 nm, and every AgNS was made up by about 20 nm silver nanoparticles, and the nanosheets were still independent in the close-packed film without agglomeration (Fig. 2a). Furthermore, the AgNS films on the cBN surfaces were not obviously changed after sonication for 5 min, indicating the strong adhesion of AgNS films to the cBN/Si(001) surfaces. Thus, the AgNS/AuNP/ NH$_2$-cBN/Si(001) film prepared by chemical deposition is extremely stable and accessible to optical investigation. In Fig. 2b, besides the reflection peaks indexed to cBN/Si(001) substrate, the reflection peaks of (111), (200), (220), and (311) were observed according to the randomness and complexity of the as-prepared sheet shapes. Owing to crystal face growth rule, to reach the state of thermodynamic stability, the crystal face with low free energies should grow more slowly and should more easily appear in large proportions.[20,21] As a result, the {111} crystal face with low free energies could be exposed in large proportions. Moreover, the citrate ions were adsorbed strongly to the {111} crystal face and restrained the crystal growth rate along the {111} crystal face. Thus, the restricted growth of the stable {111} crystal face is usually considered as
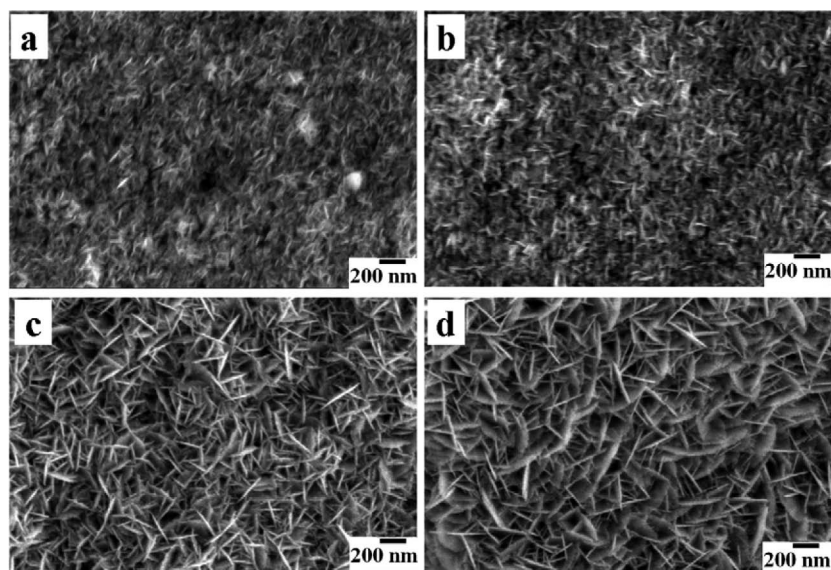
Fig. 1   SEM images obtained from the AuNP/NH$_2$-cBN/Si(001) surfaces after silver deposition for: 10 s (a), 1 min (b), 3 min (c), and 5 min (d).
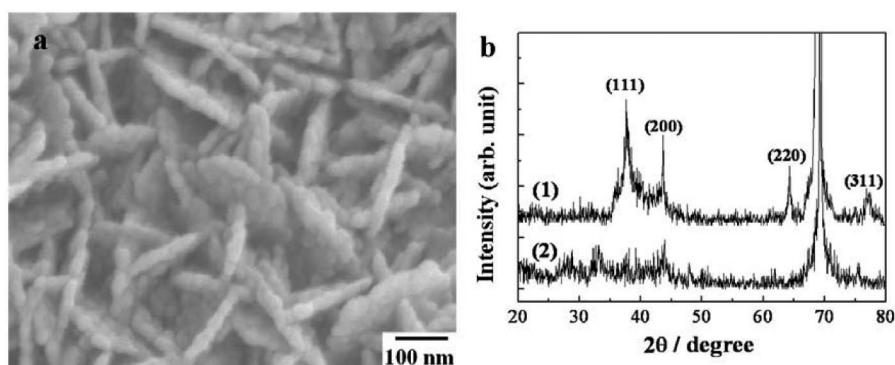

Fig. 2   (a) High-magnification SEM image of the AgNS/AuNP/NH$_2$-cBN/Si(001) surface for 5 min deposition; (b) XRD pattern obtained from the AgNS/AuNP/NH$_2$-cBN/Si(001) surface for 5 min deposition (1) and the cBN/Si(001) surface (2).

the reason for the formation of sheet-like metallic nanostructures.[22]   However, the crystal faces of {100}, {110} and {311} with high free energies easily appear on edges, corners, and protuberances, in small proportions.[20,21]   It has been reported that the enhancement of the Raman signal encountered in SERS arises mainly from so-called "hot spots" in various metallic nanostructures, and the "hot spots" exist on sharp protrusions and sites between two particles in proximity. Therefore, the existence of many sharp edges, the proximity of silver nanoparticles in every AgNS, and the cross-linked structure in the AgNS samples are expected to provide a highly SERS active substrate.

Effect of silver deposition time on the SERS activity of PATP

To confirm the high SERS activity of the AgNS/AuNP/ NH$_2$-cBN/Si(001) samples, we chose PATP as an analyte because it has been well-characterized by SERS and most of the prominent Raman bands have been assigned. Figure 3 shows a set of the SERS spectra on the AgNS/AuNP/NH$_2$-cBN/Si(001) samples with different deposition times. Noticeably, SERS intensity of PATP was dependent on the size of AgNS and the SERS intensity increased with increasing the silver deposition
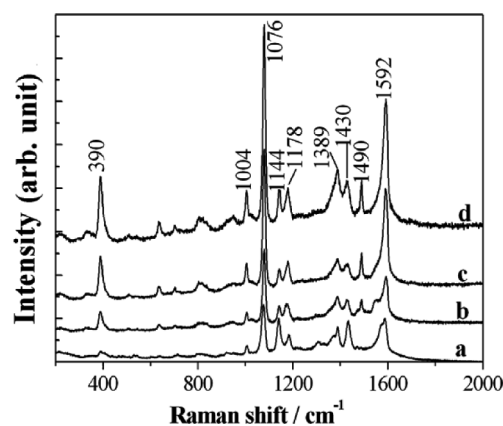

Fig. 3   SERS of 100 nM of PATP adsorbed on the AgNS/AuNP/ NH$_2$-cBN/Si(001) film with different silver deposition times: (a) 10 s, (b) 1 min, (c) 3 min, and (d) 5 min.

time. This is attributed to the facts that the AgNS/AuNP/NH$_2$-cBN/Si(001) sample with 5 min silver deposition results in the
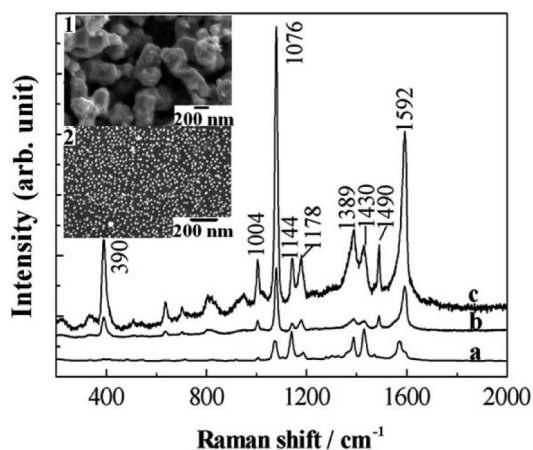
Fig. 4   SERS of 100 nM of PATP adsorbed on the cBN/Si(001) films after modification with: (a) silver mirror film, (b) AuNP/NH$_2$, (c) AgNS/AuNP/NH$_2$. Insets (1) and (2) are the SEM of the samples (a) and (b), respectively.

Fig. 5   SERS obtained from the AgNS/AuNP/NH$_2$-cBN/Si(001) films after adsorption of PATP with different concentrations: (a) 10 nM, (b) 1 nM, (c) 0.1 nM, (d) 10 nM after 1 month.

increased active sites and enhanced local electromagnetic field. The SERS intensity of PATP for the samples after 5 min silver deposition had no change, because the AgNS remained unaffected in terms of size and shape after 5 min silver deposition as described above.   As indicated in Fig. 3, the spectra of PATP obtained on the AgNS/AuNP/NH$_2$-cBN/Si(001) surface are similar to those reported by Zheng *et al*. on silver nanoparticles in colloid.[23]   The spectra are dominated with the a$_1$ vibration modes (in-plane, in-phase modes) at 1004, 1076, 1178, and 1592 cm^{-1}.   The bands at 1144, 1389, and 1430 cm^{-1} are assigned to the b$_2$ vibrational modes, and the band at 390 cm^{-1} belongs to one of the vibration modes of the C–S band, most likely the bending mode of the C–S band.   To obtain the maximum intensity of the SERS spectra, we selected the AgNS/ AuNP/NH$_2$-cBN/Si(001) sample after 5 min silver deposition for the following studies.

Comparison of SERS activity of the AgNS/AuNP/NH$_2$-cBN/ Si(001) and other substrates

For comparison, Fig. 4 shows the spectra of the PATP molecules adsorbed on the AuNP/NH$_2$-cBN/Si(001) surface (no AgNS deposition) and a silver film/cBN/Si(001) surface prepared by the mirror reaction, and the morphology of the resulting films are shown in the insets of Fig. 4.   The two samples were used as a control experiment because such films were good SERS substrates according to previous reports.[24]   The SERS spectra of PATP were observed on the above two substrates, but obviously the AgNS/AuNP/NH$_2$-cBN/Si(001) surface with 5 min deposition exhibited the highest enhancement ability.   The SERS intensity at 1076 cm^{-1} for the AgNS/AuNP/ NH$_2$-cBN/Si(001) sample is about 10 and 8 times higher than those for the AuNP/NH$_2$-cBN/Si(001) and silver film/cBN/ Si(001) by the mirror reaction, respectively.   The possible reasons for the high Raman intensity enhancement are as follows.   SERS is a very local phenomenon occurring at sharp features and large curvature regions of the rough surface.   In this case, the nanosheets, as shown in Fig. 2, mainly have sharp polyhedron morphology with distinct edges and corners.   The crystal faces of the structural features with high free energies, such as {110} and {311} crystal faces as shown in morphology analysis, can act as "hot sites" for surface plasma.   Excited by the incident radiation, a collective surface plasma is trapped
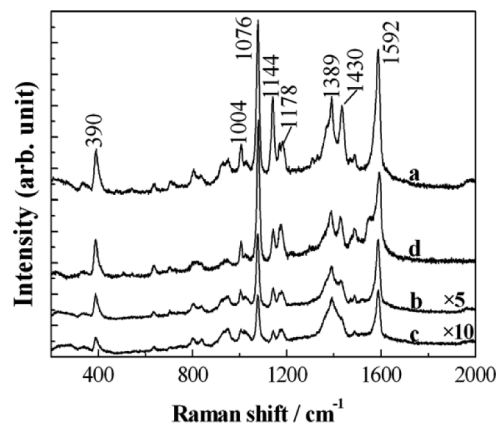
between the cross-linked nanosheets, creating a huge local electric field at these structures.   In addition, the b$_2$ vibrational modes of PATP molecules could only be selectively enhanced by the charge transfer mechanism of the metal to the adsorbed molecules.

Detection of PATP by the SERS spectra on the AgNS/AuNP/NH$_2$- cBN/Si(001) surfaces

The SERS spectra of PATP at concentrations ranging between 0.1 and 10 nM on the AgNS/AuNP/NH$_2$-cBN/Si(001) surfaces are shown in Fig. 5.   The intensity of most Raman bands decreased with decreasing concentration of PATP in the range from 10 to 0.1 nM.   The limit of detection of PATP was determined to be lower than 0.1 nM, because the spectrum of the 0.1 nM sample also has fairly good quality and the main peaks have high signal-to-noise ratios.   However, at low concentrations, the spectra became poorly resolved.   For example, a peak at 1430 cm^{-1} disappeared at the concentration below 0.1 nM.

The reproducibility and stability of the AgNS/AuNP/ NH$_2$-cBN/Si(001) substrates were also investigated by the measurement of the Raman activity to 10 nM PATP.   The relative standard deviation of the peak at 1076 cm^{-1} was 1.5 – 6.8% for 10 points on the film for 5 SERS active substrates. Figure 5 also shows the Raman spectrum of the samples after 1 month.   The peak at 1076 cm^{-1} retained about 90% of the initial SERS intensity and the main bands were still clear and unambiguous.   For comparison, the stability of the above silver film/cBN/Si(001) surface prepared by the mirror reaction was studied simultaneously.   The relative standard deviation of the peak at 1076 cm^{-1} was 5.6 – 16.7% for 10 points on the above silver film for 5 SERS active substrates, and the SERS intensity at 1076 cm^{-1} just preserved 65% of initial intensity after 1 month.   Clearly, the AgNS/AuNP/NH$_2$-cBN/Si(001) substrate showed higher stability than the silver film/cBN/Si(001) substrate prepared by the mirror reaction, which could be ascribed to the uniformity of the AgNS film and to the strong adhesion of the AgNS with the substrate.   Moreover, compared with previous reports on other substrates, such as porous Au/Ag nanostructured-modified silica films, Au nanorod-modified indium-doped tin oxide films, and μAg powders/polymers,[25-27] the higher stability obtained in present AgNS/AuNP/ NH$_2$-cBN/Si(001) can be mainly attributed to the extremely high physical and chemical stability of the cBN substrate.

Conclusions

In summary, we demonstrate that a high-density and cross-linked AgNS monolayer on cBN/Si(001) surface formed by the catalysis of AuNP is a promising candidate for SERS. Firstly, the fabrication of the AgNS/AuNP/NH$_2$-cBN/Si(001) substrate is simple. Secondly, in comparison with the AuNP monolayer film and silver film from the mirror reaction, the prepared substrate exhibited higher Raman activity. Lastly, the substrate also showed higher stability and reproducibility than other substrate prepared by other methods. Due to the above excellent performances, the prepared sample may find practical applications for routine SERS analysis, and this work represents a significant step forward in the science and technology of cBN.

Acknowledgements

References

1. K. Kneipp, H. Kneipp, I. Itzkan, R. R. Dasari, and M. S. Feld, *Chem. Rev.*, **1999**, *99*, 2957.
2. C. L. Haynes, A. D. McFarland, and R. P. V. Duyne, *Anal. Chem.*, **2005**, *77*, 338A.
3. F. Le, D. W. Brandl, Y. A. Urzhumov, H. Wang, J. Kundu, N. J. Hales, J. Aizpurua, and P. Nordlander, *ACS Nano*, **2008**, *2*, 707.
4. R. F. Aroca, R. A. Alvarez-Puebla, N. Pieczonka, S. Sanchez-Cortez, and J. V. Garcia-Ramos, *Adv. Colloid Interface Sci.*, **2005**, *116*, 45.
5. N. R. Jana and T. Pal, *Adv. Mater.*, **2007**, *19*, 1761.
6. X. Q. Zou, E. Ying, and S. J. Dong, *J. Colloid Interface Sci.*, **2007**, *306*, 307.
7. K. Kneipp, H. Kneipp, I. Itzkan, R. R. Dasari, and M. S. Feld, *J. Phys.: Condens. Matter*, **2002**, *14*, R597.
8. T. Qiu, X. L. Wu, J. C. Shen, P. C. T. Ha, and P. K. Chu, *Nanotechnology*, **2006**, *17*, 5769.
9. C. Ruan, G. Eres, W. Wang, Z. Zhang, and B. Gu, *Langmuir*, **2007**, *23*, 5757.
10. Y. C. Tsai, P. C. Hsu, Y. W. Lin, and T. M. Wu, *Electrochem. Commun.*, **2009**, *11*, 542.
11. M. L. Coluccio, G. Das, F. Mecarini, F. Gentile, A. Pujia, L. Bava, R. Tallerico, P. Candeloro, C. Liberale, F. D. Angelis, and E. D. Fabrizio, *Microelectron. Eng.*, **2009**, *86*, 1085.
12. Y. C. Tsai, P. C. Hsu, Y. W. Lin, and T. M. Wu, *Sens. Actuators, B*, **2009**, *138*, 5.
13. C. B. Samantaray and R. N. Singh, *Int. Mater. Rev.*, **2005**, *50*, 313.
14. J. Yu, Z. Zheng, H. C. Ong, K. Y. Wong, S. Matsumoto, and W. M. Lau, *J. Phys. Chem. B*, **2006**, *110*, 21073.
15. W. J. Zhang, C. Y. Chan, X. M. Meng, M. K. Fung, I. Bello, Y. Lifshitz, S. T. Lee, and X. Jiang, *Angew. Chem., Int. Ed.*, **2005**, *44*, 4749.
16. W. J. Zhang, I. Bello, Y. Lifshitz, K. M. Chan, X. M. Meng, Y. Wu, C.Y. Chan, and S.-T. Lee, *Adv. Mater.*, **2004**, *16*, 1405.
17. Y. L. Zhou, J. F. Zhi, P. F. Wang, Y. M. Chong, Y. S. Zou, W. J. Zhang, and S. T. Lee, *Appl. Phys. Lett.*, **2008**, *92*, 163105/1.
18. S. J. Park, T. A. Taton, and C. A. Mirkin, *Science*, **2002**, *295*, 1503.
19. Y.-S. Chen, A. Tal, D. B. Torrance, and S. M. Kuebler, *Adv. Funct. Mater.*, **2006**, *16*, 1739.
20. J. T. Zhang, X. L. Li, X. M. Sun, and Y. D. Li, *J. Phys. Chem. B*, **2005**, *109*, 12544.
21. L. H. Lu, A. Kobayashi, K. Tawa, and Y. Ozaki, *Chem. Mater.*, **2006**, *18*, 4894.
22. M. V. Cañamares, J. V. Garcia-Ramos, J. D. Gómez-Varga, C. Domingo, and S. Sanchez-Cortes, *Langmuir*, **2005**, *21*, 8546.
23. Q. Zhou, Q. Fan, Y. Zhuang, Y. Li, G. Zhao, and J. W. Zheng, *J. Phys. Chem. B*, **2006**, *110*, 12029.
24. Y. Saito, J. J. Wang, D. A. Smith, and D. N. Batchelder, *Langmuir*, **2002**, *18*, 2959.
25. L. H. Lu, A. Eychmüller, A. Kobayashi, Y. Hirano, K. Yoshida, Y. Kikkawa, K. Tawa, and Y. Ozaki, *Langmuir*, **2006**, *22*, 2605.
26. X. G. Hu, W. L. Cheng, T. Wang, Y. L. Wang, E. Wang, and S. J. Dong, *J. Phys. Chem. B*, **2005**, *109*, 19385.
27. K. Kim, H. K. Park, and N. H. Kim, *Langmuir*, **2006**, *22*, 3421.